Available online at www.sciencedirect.com
ScienceDirect
Diamond & Related Materials 17 (2008) 925–930
DIAMOND AND RELATED MATERIALS
www.elsevier.com/locate/diamond

Evolution of the opto-electronic properties of amorphous carbon films as a function of nitrogen incorporation

F. Alibart [a], O. Durand Drouhin [a], M. Lejeune [a], M. Benlahsen [a,*], S.E. Rodil [b], E. Camps [c]

[a] *Laboratoire e Physique de la Matière Condensée, 33 rue Saint Leu, 80000 Amiens France*
[b] *Instituto de Investigationes en Materiales, Universidad Nacional Autónoma de México, México D.F. 04510, México*
[c] *Instituto Nacional de Investigaciones Nucleares, Apdo. Postal 18-1027, México D.F 11801 México*

Received 16 November 2007; received in revised form 16 January 2008; accepted 22 January 2008
Available online 8 February 2008

Abstract

The present work provides correlations between the optical, electronical and microstructural properties of amorphous carbon nitride films (a-CN_x) deposited by Direct Current (DC) magnetron sputtering technique versus the $N_2/Ar+N_2$ ratio. The microstructure of the films was characterized by Raman spectroscopy and optical transmission measurements. The evolution of both the density of states (DOS) located between the bandtail states and the density of states around the Fermi level $N(E_f)$, have been investigated by electrical measurements versus temperature varying the $N_2/Ar+N_2$ ratio. The evolution of the microstructure versus N reveals a continuous structural ordering of the sp^2 phase, which is confirmed by the optical and the conductivity measurements. The conductivity variation was interpreted within the framework of the band structure model of the π electrons in a disordered carbon with the presence of localized states.

Keywords: Carbon nitride films; Raman spectra; Electrical and electronic properties

1. Introduction

Motivated by the elaboration of the β-C_3N_4 phase predicted theoretically by Liu and Cohen [1], amorphous carbon nitride films (a-CN_x) have given rise to a large variety of films deposited by numerous techniques [2]. The poor success in the realisation of these attempts have nevertheless produced films with different mechanical behaviours, from smooth to hard coatings, and a wide range of opto-electronic properties, from insulating to semi-metallic. In this way, a-CN_x thin films are now being considered as a possible material to extend the applications of amorphous carbon materials which have presented limited success in electronic devices (OLEDs, TFTs…). The performance of such devices depends on the electronic properties of the films [3–6].

The large changes of the electronic properties of carbon nitride films can be connected to the ability of nitrogen to bond to C in diverse ways; which include the sp^3 (tetrahedral, C–N), sp^2 (trigonal, C=N) and the chain terminating sp^1 linear (–C≡N and –N≡C bonds) [7,8]. A general picture is that the electrical properties of amorphous carbon (a-C) films, whether hydrogenated or not, are dominated by π states of sp^2-hybridized carbon atoms because the σ states of sp^2- and sp^3-hybridized carbons are further away from the Fermi level and the Csp^2 clusters control the opto-electronic properties [9–12]. It is known that π states of sp^2 carbon atoms form tail states that are linked with valence- and conduction-band edges and contribute to the density of states (DOS) in the gap. The proportion of Csp^2 atoms and their arrangement in smaller or larger clusters determine the optical gap and have a significant influence on the electrical transport as well [9,10]. It is, therefore, very important to understand the correlation between the microstructure of the films and their electrical conduction.

Since the microstructure of a-CN_x films is strongly dependent on the deposition conditions, in this paper, we investigated the opto-electronic properties of a-CN_x thin films deposited by Direct Current (DC) magnetron sputtering technique versus the N content, and relate them to the bonding structure of the films. The used deposition technique is known to produce highly sp^2

* Corresponding author.
E-mail address: mohamed.benlahsen@sc.u-picardie.fr (M. Benlahsen).

0925-9635/$ - see front matter © 2008 Elsevier B.V. All rights reserved.
doi:10.1016/j.diamond.2008.01.080

materials due to the low energy and low ion densities involved during the deposition. The objective of this work is to develop improved procedures for the deposition and characterization in order to improve the electronic properties of the a-CN_x films.

2. Experimental details

The a-CN_x thin films were deposited using a DC magnetron sputtering from a high purity (99.999%) graphite target in a high vacuum chamber on corning glass and intrinsic silicon substrates at room temperature. The pressure during deposition was kept constant at 1.3 Pa, the DC power was fixed at 200 W and the deposition time at 10 min at the substrate temperature close to 50 °C. The films were elaborated using a plasma gas (N_2/Ar) mixture. The $N_2/Ar+N_2$ ratio was varied between 0 and 10% in order to vary the N content into the materials. The relation between the percentage of nitrogen gas in the mixture (i.e. the $N_2/Ar+N_2$ ratio) and the solid phase composition (N/C+N) ratio, e.g. given by XPS has been studied in the literature. It was reported that for $N_2/Ar+N_2$ ratio <30%, the N content in the film increases monotonically versus the $N_2/Ar+N_2$ ratio [13–15]. The thickness of the samples was measured using a Dektak 3st profilometer and observed to increase monotonously from 190 to 360 nm when increasing the N_2 content into the plasma.

The optical gap was determined by optical transmission measurements, in the 300–3000 nm range using a Varian *Cary 5* spectrometer in reflection and transmission mode. Raman spectra were performed at room temperature using an Ar laser of wavelength 1064 nm. The laser power was limited to 50 mW in order to prevent any material heating and structural modification. The electrical conductivity measurements were conducted by a computer-controlled Keithley 6517A electrometer under controlled argon atmosphere at constant heating rate on the order of 2 K/min, in the coplanar configuration of platinum electrodes on samples deposited on glass substrates, for temperature ranging from 110 to 423 K. The 60 nm thick platinum electrodes, having a circular configuration to avoid leakage currents, were sputtered on the glass substrates samples and the ohmic contact verified by I(V) measurements.

3. Results and discussions

Raman spectroscopy is probably the most common technique for the evaluation of carbon films. The spectra of all samples are very similar, and exhibit a very broad peak centred around 1550 cm^{-1} (corresponding to the *G* line associated with the optically allowed E_{2g} zone centre mode of crystalline graphite) and a barely observed peak centred around 1350 cm^{-1} (corresponding to the *D* line associated with the breathing mode of aromatic structures) [16–19]. The *G* peak arises from vibrations of all sp^2 sites and in both olefinic chains and aromatic rings, while the existence of a *D* peak indicates the presence of aromatic six fold rings [19]. The position, the full width at half maximum of the *D* (ΔD) and *G* (ΔG) bands and the integrated intensity ratio (I_D/I_G), can be used as indicators of the carbon bond arrangements [16–20]. We performed a computed deconvolution of the experimental Raman spectra in order to increase the accuracy of the estimation of these parameters using a Gaussian profile at the *G* and *D* positions after a background correction.

We represent on Fig. 1(a, b) the variation of the I_D/I_G ratio and the *G* peak position versus the $N_2/Ar+N_2$ ratio. In the same trend as the previous results, both the I_D/I_G ratio and the *G* peak position increase for an increase of the $N_2/Ar+N_2$ ratio from 0 to 3%. The increase of *G* peak position (Fig. 1-a) toward the value of $G_{graphit}$ peak position reveals a "graphitisation" of the films. This "graphitisation" can occur due to two main processes: the increase of the Csp^2 comparatively to the Csp^3 bonds but also from an "ordering" of the Csp^2 domains. Since the DC technique produces films which are mainly sp^2 bonded [21], the important shift of the *G* peak from 1520 to 1540 cm^{-1} has been attributed mainly to an ordering of the Csp^2 domains. This idea was supported by the decrease of the ΔG peak, in the same region of the $N_2/Ar+N_2$ ratio, suggesting an ordering of the Csp^2 clusters into the global network. The saturation of the *G* band position at 1540 cm^{-1} reflects the maximum possible Raman shift for C atoms bonded in sp^2 rings (noting that higher Raman shifts are possible for sp^2 C atoms found in chains, with shorter bond lengths). The segregation of the Csp^2 atoms is currently described by the so-called two-phase or cluster model [9]. Indeed,

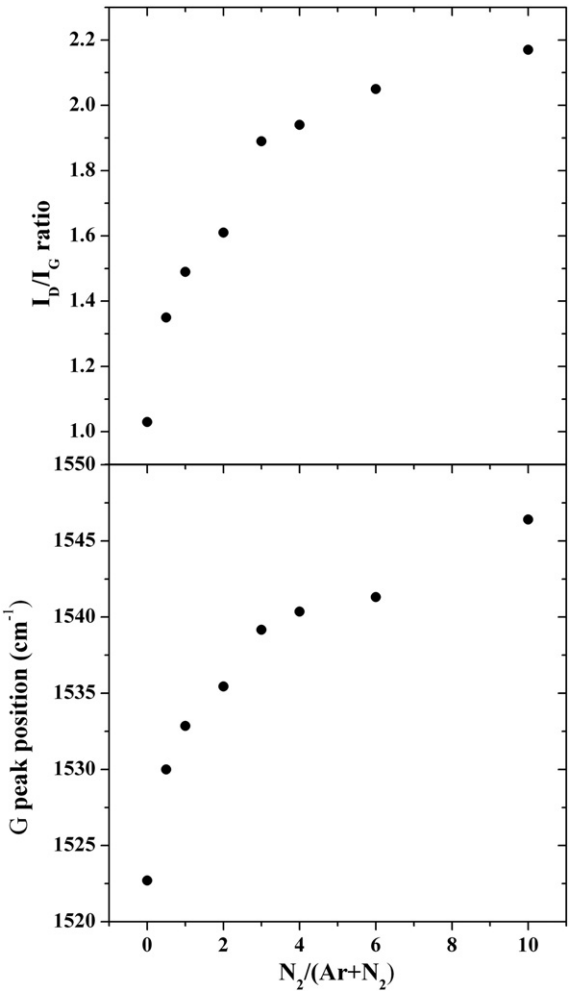

Fig. 1. (a, b) The variation of G peak position (a) and the I_D/I_G ratio (b) versus the $N_2/Ar+N_2$ ratio.

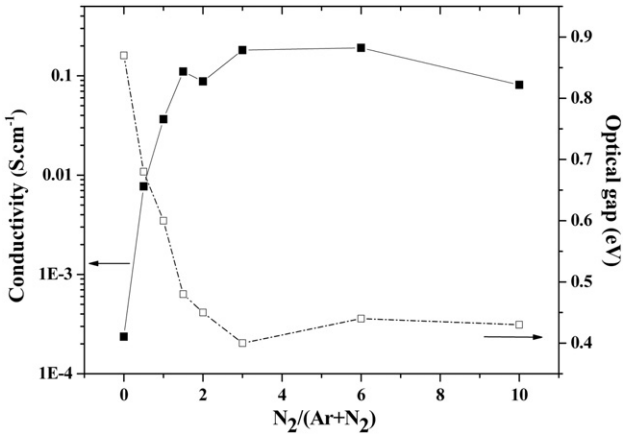

Fig. 2. The evolution of optical gap and electrical conductivity at room temperature (σ_{RT}) versus the $N_2/Ar+N_2$ ratio. The line is only a guide for the eyes.

the Csp^2 hybridized carbon atoms, for energetic reasons, tend to pair up and to make double bonds, then to gather into more or less extended π-bonded clusters based on nm-sized clusters in the form of graphitic rings or olefinic chains giving rise to π and π* bands. The increase of the I_D/I_G ratio from 1 to 1.9 when the $N_2/Ar+N_2$ ratio varies between 0 and 3% (Fig. 2) can be directly linked to an increase of the sp^2 domain size (i.e. an increase of the number of rings into the cluster) [18,19]. For higher values of the $N_2/Ar+N_2$ ratio.

The observed saturation of the I_D/I_G ratio versus the $N_2/Ar+N_2$ ratio (Fig. 1-b) might be explained by the microstructure changes due to the N incorporation within the films. Indeed, the incorporation of nitrogen breaks the long-range order of the graphitic structure and promotes both the clustering of Csp^2 sites and the disorder in theses ring structures. Indeed, when *N* is introduced into a carbon network, the CN vibration frequencies for chain-like molecules and ringlike molecules are very close to those of pure carbon. The modes are delocalized over both C and N sites due to the capability of N to acquire the same hybridizations as C atoms. In addition, with increasing the nitrogen content most of the network becomes terminated by NH or $CNsp^1$ (i.e. (C≡N)) bonds, which may terminate a chain or form part of network within film the structure of the films and determines the extent of the void structure limiting the cluster size increase [6–8,14,21,22]. This result suggests that even if nitrogen has an important role in the enlargement of the sp^2 domains, this role is limited to the low ratio in the plasma gas mixture (below 3%). For higher nitrogen content, the Raman features can be connected to the appearance of polymeric features such as olefinic N-containing chains, rather than aromatic environments, and to the transition from a dense material to a less dense and more ordered alloy as it was reported in the literature [6,21]. So, our results suggest that beside the transition to Csp^2, the disorder of the C–C network is enhanced with increasing $N_2/Ar+N_2$ as suggested by the I_D/I_G ratio which, exhibits a similar tendency and suggests the increase both in the graphite size and number of the graphitic Csp^2 clusters: the translation periodicity of the atomic network of the solid is disturbed by bond-angle distortions and particle size effects caused by the nitrogen incorporation on the carbon structure. These results suggest some evolution in the density of the states (DOS) of the a-CN_x layers. But, direct links between microstructure and the DOS cannot be so easily established. In order to find a connection between these two properties, we studied the optical and electronic properties [23,24].

The evolution of optical gap and electrical conductivity at room temperature (σ_{RT}) versus $N_2/Ar+N_2$ ratio are shown in Fig. 2. Below 3%, the observed decrease of the optical gap E_g can be connected to an increase of the sp^2 domains size in agreement with the Raman results reported above, and can be related to electronic transitions between extended states, i.e. the π/π* transitions, that come from sp^2 domains, in which the electronic wavefunctions appears delocalised. Thus, the decrease of E_g due to nitrogen incorporation into the network was also correlated to an increase of the π/π* contribution [6,21–24]. We can notice that the gap values observed in our samples were in agreement with a mainly sp^2 bonded carbon materials. For higher $N_2/Ar+N_2$ ratio, the gap values remained nearly constant in agreement with the Raman results presented above, which suggest that for $N_2/Ar+N_2$ ratios above 3%, the structural changes introduced by N are more subtle.

The electrical conductivity is the second physical characteristic that is determined by the DOS of the material, as observed by the evolution of the conductivity shown in Fig. 2. Indeed, the electrical transport properties of amorphous carbons are governed by the π states of the sp^2 sites and their distribution because they form the valence and conduction band edges [9]. π bonding at sp^2 sites are very sensitive to these medium-range correlations due to their delocalized nature [9,25–27]. The presence of a distribution of cluster sizes, which is certainly the case in carbon nitride, will therefore induce strong symmetric fluctuations of the valence and the conduction band edges over distances which correspond to several atoms (medium-range fluctuations). Three conduction mechanisms have been proposed to explain the electrical conductivity in amorphous carbon materials (i) the conduction in extended states, (ii) the conduction in band tails and, (iii) the conduction in localized states at the Fermi level [25–28]. As it was reported, all the sp^2 configurations are associated to localized states that can be either strongly localized (states around the Fermi level) or weakly localized (states in the π/π* bands edges), i.e. the wavefunction of each state is spatially limited and can be located at a different energy level into the density of the states (DOS). When the density of states $N(E_i)$ around an energy level E_i increases, the distance between the associated states decreases and becomes close to the localisation length of the electronic wavefunction creating extended states. The extended states of the π/π* bands are an illustration of this idea. Assuming this approach, the DOS of the mainly sp^2 a-CN_x thin films has been described using the Mott's model [29,30]. The π/π* bands come from sp^2 domains in which the electrons are spatially delocalised. So, the states between these two bands can be either in the bandtail or around the Fermi level. The correlation between the optical gap results and electrical conductivity measurements can well be described by the DOS shape [6,31].

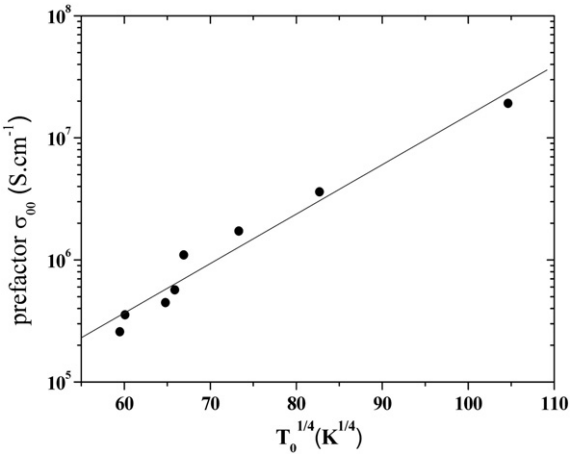

Fig. 3. Relationship between the parameters σ_{00} and $T_0^{1/4}$ in the ohmic regime.

It is now accepted that the optical gap (E_g) in amorphous carbon films is attributed to the transitions between weakly localised states of the π/π* states that come from the sp^2 clusters [9–12,24]. The π states are therefore expected to control the band edges, and therefore the value of the gap of this material. These variations are well explained by the cluster model [9]. Each sp^2 C cluster is characterized by a local gap determined by the π states, which will depend on the size, and probably also on the nature (ring- or chain-like) and on the distortions of this cluster [9,22,24]. The increase of σ_{RT} has been observed to vary in an opposite trend than the gap values. The increase of conductivity, below 3%, is consistent with the continuous narrowing of the G band and to the I_D/I_G ratio evolution (the increase of size of the sp^2 domains). The increase of size of the sp^2 domains allowed the electron to move over a greater distance via extended states in the samples. In the second region of N incorporation ($N_2/Ar+N_2$ ratio from 3–10%), the samples did not show significant changes in σ_{RT} and gap measurements.

On the other hand, the evolution of conductivity versus temperature clearly showed two regimes; between 110–300 K and 300–450 K, respectively. At low temperatures, the conductivity trend showed an almost linear dependence on $1/T^{1/4}$, revealing that the carrier transport in the film was dominated by variable-range hopping (VRH) conduction with a semiconducting character in the presence of local disorder. The conduction by tunneling or phonon-assisted hopping between localized states, rather than through propagation in extended states, is expected throughout a broad range of temperatures for the deposited films. Charge carriers are likely to be localized throughout the entire range of the sp^2 clusters and the dangling bond states within the band gaps associated with sp^2 and sp^3 sites. Assuming that our materials can be described in the framework of sp^2 domains where the electrons appears delocalised through them, the VRH conduction is expected to occur between each sp^2 domains. According to Godet et al. [6,32–34], the VRH conduction can occur between states located at the Fermi level (Mott's theory) or between states located in the bandtail (Bandtail Hopping Theory). Both states are located between the π/π* bands. From the fit of σ versus $1/T^{1/4}$, we can extract two parameters, σ_{00} and $T_o^{1/4}$ that come from the VRH model equation:

$$\ln\sigma = \ln\sigma_{00} - \left(\frac{T_0}{T}\right)^{1/4}.$$

A positive correlation between σ_{00} and $T_o^{1/4}$ is due to bandtail hopping whereas a negative or constant correlation is attributed to hopping conduction around the Fermi level [29]. We present in Fig. 3 the positive correlation between σ_{00} and $T_o^{1/4}$ found in our series of samples, which allows us to connect the VRH to bandtail hopping in the present study. In the case of bandtail hopping, a relevant criterion to study the VRH conduction is the localisation parameter (LP) defined as $LP = N(E_f).\gamma^{-3}$ (eV^{-1}) where $N(E_f)$ is the density of states around the Fermi level and γ^{-1} is the localisation radius of the electronic wave functions. As mentioned by Godet et al. [32], the dimensionless of LP values can be extract assuming $N(E_f).\gamma^{-3} = 310$ in the case of bandtail hopping. These two physical parameters cannot be separated and the increase of conductivity due to VRH is associated to an increase of the LP value [6,32–34]. The increase of LP in the first region of the N_2 content into plasma, as shown in Fig. 4, was in good agreement with the increase of σ_{RT} and suggested the contribution of conduction through localized states (VRH).

The electrical conductivity versus temperature in the 300–473 K region can bring further information about the DOS evolution, more precisely, about the states located between the π/π* bands. An interesting result is deduced from the Arrhenius plot of the conductivity σ versus the inverse of the temperature ($1/T$), which reveals a thermally activated process associated with an activation energy (E_a) attributed to different electronic transitions between occupied and empty states. In the theory of amorphous semiconductors [30], two types of thermally activated transitions can occur: the first one (corresponding to the lowest energy E_a) come from transitions between the Fermi level and the localised defect band (either π or π*) states and the second one, from the Fermi level to the π* band. The transitions from the π band to the π* band are usually attributed to optical transitions and are inaccessible by thermal activation [9,11,27].

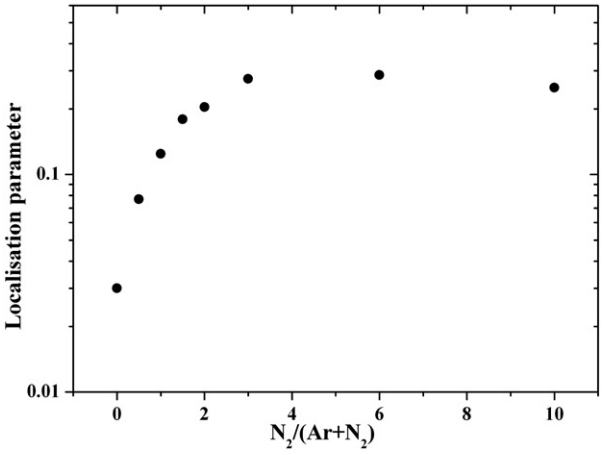

Fig. 4. The variation of the localisation parameter (LP) versus $N_2/Ar+N_2$ ratio.

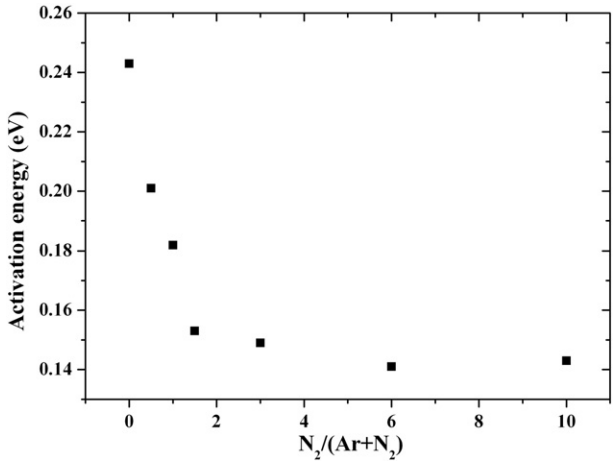

Fig. 5. The variation of the activation energy (E_a)) versus the $N_2/Ar+N_2$ ratio.

We reported in Fig. 5 the activation energy observed in the 300–473 K region. We have reported in precedent studies that no structural changes can occur in the deposited a-CN_x films in the range of the studied deposition temperature (50 °C) [35,36]. The first structural modification observed around 200 °C has been associated to the evolving gases as CO_2 and CO suggesting the post-deposition contamination of the films by oxygen [35]. In the first region (below 3%), the higher values of the optical gap (0.9 to 0.4 eV) compared to those of E_a (0.24 to 0.14 eV) allow us to connect E_a to the defects evolution, due to the different bonding configurations of the CN bonds. So, the obtained activation energy cannot be attributed to transitions between the Fermi level and the π^* band but to the first mechanism: transitions between the Fermi level and localized bandtails states. Moreover, the decrease of E_a as the N_2 fraction increased suggests a larger overlapping of the π/π^* bands near the Fermi level as a result of a higher density of defects in the samples [27]. So the increase of sp^2 cluster size, suggested by Raman, is associated with a greater delocalization of the unpaired electrons as the cluster size increases which caused the "graphitisation" of the C network. At relatively low levels of nitrogen content, below 3%, the nitrogen will introduce additional states located either around the Fermi level or in the bandtail, decreasing the activation energy, E_a. The resulting variation of the E_g and the electrical properties can be correlated to the lattice vibrations leading to the scattering of charge carriers by the N atoms and the more disorder nature of the C films [21]. This result is qualitatively in accordance with the LP variation but we cannot evaluate quantitatively the evolution of the states located into the gap. For the higher values of $N_2/Ar+N_2$ ratio above 3%, the constant behaviour of E_a for the samples was in agreement with the previous results: the N incorporation did not induce changes in this region for both the sp^2 domains (associated to the π/π^* transitions) and to states located into the gap and observed in the VRH results.

4. Conclusion

To summarize, the interpretation presented in this study has allowed to link the optical measurements to the electrical ones and to evaluate the DOS evolution with N incorporation for highly sp^2 materials such as DC sputtering carbon nitride thin films. The analysis of the π/π^* bands versus $N_2/Ar+N_2$ ratio reveal two regions:

- From 0 to 3%, the N incorporation induces the increase of sp^2 domains size in the film (the "graphitisation" of the C network), which is associated with greater delocalization of the unpaired electrons. In addition, N introduces additional states located either around the Fermi level or in the bandtails, decreasing the E_a.
- From 3 to 10%, no significant changes of the E_g and the electrical properties were observed suggesting that the sp^2 domains did not present any evolution in size or ordering, as also suggested by the analysis of the Raman spectra. The N incorporation did not induce modification on the states located into the gap (i.e. no deep changes on the physical properties for the samples were observed).

Acknowledgements

We would like to thank S. Muhl and C. Godet for the helpful discussions.

References

[1] A.Y. Liu, M.L. Cohen, Science 245 (1989) 841.
[2] H. Sjöström, S. Stafström, E. Broman, J.-E. Sundgren, Phys. Rev. Lett. B 75 (1995) 1336.
[3] A. Lagrini, C. Deslouis, H. Cachet, M. Benlahsen, S. Charvet, Electrochem. Commun. 6 (2004) 245.
[4] G.A.J. Amaratunga, S.R.P. Silva, Appl. Phys. Lett. 68 (1996) 2529.
[5] Somnath Bhattacharyyaa, S.R.P. Silva, App. PhyS. Lett. 90 (2007) 082105.
[6] C. Godet, N.M.J. Conway, J.E. Bourée, K. Bouamra, A. Grosman, C. Ortega, J. Appl. Phys. 91 (2002) 4154.
[7] A.K.M.S. Chowdhury, D.C. Cameron, M.S.J. Hashmi, Thin Solid Films 332 (1998) 62.
[8] M. Lejeune, O. Durand-Drouhin, S. Charvet, A. Grosman, C. Ortega, M. Benlahsen, Thin Solid Films, 444, 1-2, 1 (2003)1.
[9] J. Robertson, E.P. O'Reilly, Phys. Rev. B 35 (1987) 2946;
J. Robertson, Diamond Relat. Mater. 4 (1995) 297.
[10] C. Oppedisano, A. Tagliaferro, Appl. Phys. Lett. 75 (1999) 3650.
[11] S.R.P. Silva, J. Robertson, G.A.J. Amaratunga, B. Rafferty, L.M. Brown, J. Schwan, D.F. Franceschini, G. Mariotto, J. Appl. Phys. 81 (1997) 2626.
[12] T. Katsuno, S. Nitta, H. Habuchi, V. Stolojan, S.R.P. Silva, Appl. Phys. Lett., 85 (14) (2004) 2803.
[13] N.E. Derradji, M.L. Mahdjoubi, H. Belkhir, N. Mumumbila, B. Angleraud, P.Y. Tessier, Thin Solid Films 482 (2005) 258.
[14] S. Muhl, J.M. Mendez, Diamond Relat. Mater. 8 (1999) 1809.
[15] R. Pintaske, Th. Welzel, M. Schaller, N. Kahl, J. Hahn, F. Richter, Surf. Coat. Technol. 90 (1997) 275.
[16] D. Beeman, J. Silverman, R. Lynds, M.R. Anderson, Phys. Rev. B 3 (1984) 870.
[17] M.A. Tamor, W.C. Vassell, J. Appl. Phys. 76 (1994) 3823.
[18] F. Tuinstra, J.L. Koenig, J. Chem. Phys. 53 (1970) 1126.
[19] A.C. Ferrari, J. Robertson, Phys. Rev. B 61 (2000) 14095.
[20] G. Messina, A. Paoletti, S. Santangelo, A. Tagliaferro, A. Tucciarone, J. Appl. Phys. 89 (2001) 1053.
[21] A.C. Ferrari, S.E. Rodil, J. Robertson, Phys. Rev. B 67 (2003) 155306.
[22] M. Lejeune, O. Durand-Drouhin, K. Zellama, M. Benlahsen, Solid State Commun. 120 (2001) 337.
[23] J. Tauc, in: F. Abelès (Ed.), Optical Properties of Solids, Amsterdam, North Holland, 1972, p. 277.

[24] J. Robertson, Philos. Mag. Lett. 57 (1988) 143.
[25] C.W. Chen, J. Robertson, J. Non-Cryst. Solids 227–230 (1998) 602.
[26] H. Hofsäss, Amorphous Carbon: State of the Art, World Scientific, Singapore, 1998, p. 296.
[27] D. Dasgupta, F. Demichelis, A. Tagliaferro, Philos. Mag. B 63 (1991) 1255.
[28] R.U.A. Khan, S.R.P. Silva, Int. J. Mod. Phys. B 14 (2000) 195.
[29] N.F. Mott, Philos. Mag. 19 (1969) 835.
[30] N.F. Mott, E.A. Davis, Electronic Processes in Non-Crystalline Materials, second ed. Oxford University Press, 1979.
[31] M.A. Monclus, D.C. Cameron, R. Barklie, M. Collins, Surf. Coat. Technol. 116–119 (1999) 54.
[32] C. Godet, Philos. Mag., B 81 (2001) 205.
[33] C. Godet, G. Adamopoulos, S. Kumar, T. Katsuno, Thin Solid Films 482 (2005) 24.
[34] C. Godet, J. Non-Cryst. Solids 229-302 (2002) 299.
[35] M. Lejeune, M. Benlahsen, Diamond Relat. Mater. 17 (2008) 29.
[36] M. Lejeune, S. Charvet, A. Zeinert, M. Benlahsen, J. Appl. Phys. 103 (2008) 013507.